Journal of Materials Chemistry A

PAPER

View Article Online
View Journal | View Issue

Cite this: J. Mater. Chem. A, 2019, 7, 6038

A fast and stable Li metal anode incorporating an Mo_6S_8 artificial interphase with super Li-ion conductivity†

Ke Lu,[a] Siyuan Gao,[a] Robert J. Dick,[b] Zain Sattar[a] and Yingwen Cheng *[a]

Received 27th December 2018
Accepted 7th February 2019

DOI: 10.1039/c8ta12450g

rsc.li/materials-a

The poor interfacial stability of Li metal leads to formation of unstable solid-electrolyte interphases (SEIs) and severely limits its practical applications. Protecting Li metal with an artificial SEI that has balanced stability, conductivity and mechanical strength is critical. Here we demonstrate a design strategy for stabilizing Li using Mo_6S_8/carbon artificial SEI films. These films are directly coated on Li foil and the Mo_6S_8 particles provide ordered conduction channels for fast but regulated Li-ion flux, and provide hybrid anodes that have nearly four times higher exchange current densities. They also have seamless contact with Li metal and protect it from parasitic reactions, and hence significantly improve its stability. Consequently, Li metal batteries in which the hybrid anodes were paired with $LiNi_{0.8}Mn_{0.1}Co_{0.1}O_2$ cathodes (3.0 mA h per cell) exhibited significantly improved cycling stability (63% *vs.* 25% retention) and a stabilized Li interphase compared with pristine Li anodes.

Li metal is commonly considered as the ultimate anode material for high energy density batteries because of its unique properties particularly its highest theoretical capacity of 3860 mA h g^{-1}, low density of 0.59 g cm^{-3}, and low electrochemical potential (−3.040 V *vs.* the standard hydrogen electrode).[1–3] Unfortunately, Li metal has extremely high reactivity with almost all battery electrolytes and produces solid-electrolyte interphases (SEIs) that are unstable, nonuniform and have low Li-ion conductivity. The formation of an SEI causes irreversible loss of battery materials and fluctuations in local current densities and Li ion concentrations,[4–6] which results in substantial polarization increases and Li corrosion along with dendrite growth during Li plating and stripping.[7] Consequently, current Li anodes suffer severely from low coulombic efficiency and poor cycling stability, especially in carbonate-based electrolytes that are compatible with current 4 V intercalation cathodes.[8,9]

Modifying SEI properties with artificial protection layers recently appeared as an attractive approach to address the instability issue.[10] The composition and structure of these layers, in principle, could be tuned precisely to allow seamless contact with Li metal and provide simultaneously improved interfacial stability and balanced electronic/ionic conductivity that are required for stable battery cycling. Artificial SEI films composed of LiF,[11,12] Li-metal alloys,[13–15] nitrides,[16] cross-linked polymers,[8] Li_3PS_4,[17] and Li_3PO_4 (ref. 18) have been described. Notably, these are usually ultrathin films that are coated on Li metal through separate *in situ* reactions by immersing Li in a liquid solution that contains reactive precursors.[13,14,19–21] These coatings have been shown to be effective at suppressing side-reactions and dendrite growth, particularly under low current conditions and during the initial stages of cycling. However, they usually have limited Li-ion conductivity and/or poor flexibility, and could crack during cycling. Overall, it is still very challenging to design SEI films that could be directly coated on Li metal and afford their stable operation.[22]

Herein, we describe a new strategy of designing transferrable artificial SEI layers and demonstrate their remarkable capability for providing substantially improved interfacial stability to Li metal (Fig. 1a). These artificial layers was based on Chevrel phase Mo_6S_8/carbon composites, which are known for superior ionic conductivity and outstanding stability.[23,24] We hypothesized that artificial layers designed with robust materials that allow rapid Li-ion diffusion could effectively protect Li metal from side-reactions without sacrificing the stripping/plating kinetics, and the use of transferrable films allows for precise thickness and composition control and facilitates scalable production of hybrid anodes.[22] We discovered that the protected hybrid anodes have substantially increased Li-ion transport kinetics along with outstanding surface stability under aggressive cycling conditions. As a result of the stabilized Li surface without parasitic reactions, prototype Li metal batteries employing high loading $LiNi_{0.8}Mn_{0.1}Co_{0.1}O_2$ (NMC-811) cathodes exhibited drastically enhanced cycling stability in a carbonate electrolyte compared with unmodified Li anodes.

[a]Department of Chemistry and Biochemistry, Northern Illinois University, DeKalb, IL 60115, USA. E-mail: ycheng@niu.edu

[b]Department of Science, Trine University, Angola, IN 46703, USA

† Electronic supplementary information (ESI) available: Complete experimental details and additional characterization results, including supplemental Fig. S1–S12. See DOI: 10.1039/c8ta12450g

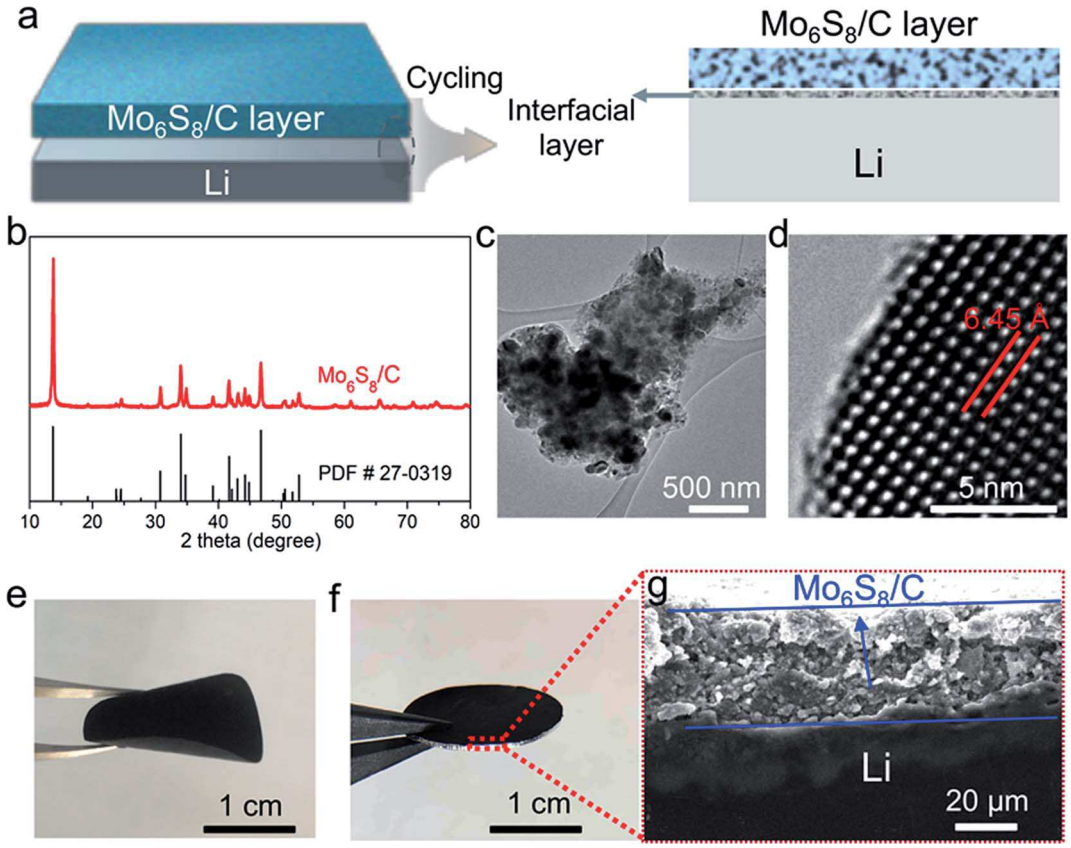

Fig. 1 (a) Schematic illustrations of protecting Li metal with Mo_6S_8/C artificial SEI layers and (b–g) structural characterization of Mo_6S_8 particles and the hybrid anodes: (b) X-ray diffraction pattern and (c and d) TEM images of the Mo_6S_8/C composite; photographs of (e) a piece of Mo_6S_8/C thin film and (f) protected hybrid Li metal anode; (g) SEM image of the interphase between the Mo_6S_8/C layer and Li metal that shows their intimate contact without separation.

Chevrel phase Mo_6S_8/carbon composites were obtained by acid leaching of Cu^{2+} off $Cu_2Mo_6S_8$/carbon, which was synthesized from precursors including 0.6 g carbon, 3.0 g MoS_2, 1.8 g Mo and 1.2 g CuS. These precursors were first ball-milled and then calcined under Ar at 1000 °C for 10 h (detailed in ESI†). Pristine Mo_6S_8 particles without carbon were also synthesized for comparison. It should be noted that this method is more scalable, faster and requires less work for producing high quality Chevrel phase compounds compared with typical methods.[25–27] The combined XRD and TEM characterization confirmed nearly 100% production of Mo_6S_8 both for the synthesis with (Fig. 1b and c) and without (Fig. S1 and S2†) carbon but particles synthesized with carbon have a smaller size and better conductivity, which are beneficial for faster ion transport necessary for improving battery operations.[26] Mo_6S_8 has inherent large open channels (~6.45 Å, Fig. 1d) between nearby clusters, which are ideal for stable and fast diffusion of a variety of cations.[23,26] When used as a host for insertion of Li^+, it delivered a specific capacity of 112 mA h g^{-1} at 0.1C and retained ~66% of the this capacity when the rate was increased to 20C in the voltage range of 1.5–2.9 V, along with superior stability (Fig. S3†).

Thin films composed of Mo_6S_8/C or Mo_6S_8 particles were prepared using polytetrafluoroethylene (PTFE) as the binder. These films (Fig. 1e) had thicknesses of ~40 μm and areal densities of ~3.5 mg cm^{-2}, and they were pressed onto the surface of bulk Li anodes (450 μm thickness) at 500 psi using a hydraulic press (Fig. 1f). The SEM image reveals that the Mo_6S_8 film and Li metal had seamless intimate contact without separation (Fig. 1g). These hybrid anodes were first assembled into coin cells using 1.0 M $LiPF_6$ in EC/DEC for evaluation of Li ion transport properties and interfacial stabilities. The direct contact of Mo_6S_8 with Li metal in the presence of electrolyte leads to rapid Li-ion diffusion to the Mo_6S_8 framework, in a way similar to battery short-circuit, and results in formation of Li-ion conductive lithiated $Li_xMo_6S_8$. The value of x was estimated as 16 based on the discharge capacity of the Li||Mo_6S_8 cells to 0.0 V (Fig. S4†). The exact structure of the fully discharged product $Li_{16}Mo_6S_8$ is complex but XRD analysis suggests dominance of the Chevrel phase crystal structure (Fig. S5†). The hybrid anodes were actually $Li_{16}Mo_6S_8$ coated Li metal. We reason that the $Li_{16}Mo_6S_8$ layer has better interfacial stability compared with pristine Li and provides three-dimensional channels for fast and regulated Li-ion flux that regulate Li stripping and plating, which is critical for mitigating formation of dendritic structures and improving SEI stability (Fig. 1a).

The Li ion plating/stripping properties of the hybrid Li anodes were evaluated using symmetric coin cells. Fig. 2a compares the cyclic voltammograms (CV) of different anodes

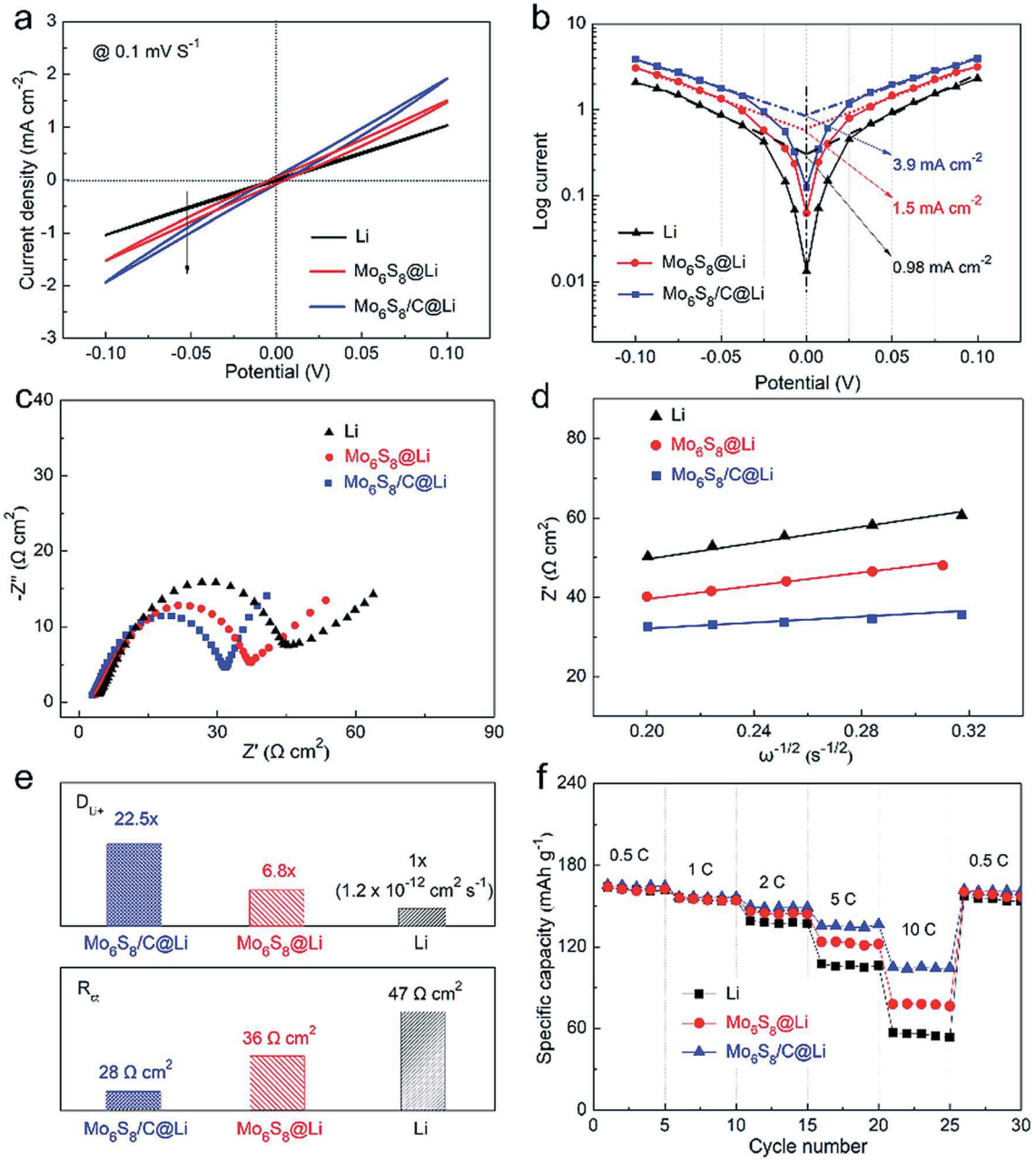

Fig. 2 Mo_6S_8/C@Li hybrid anodes have enhanced Li-ion transfer kinetics: (a) cyclic voltammogram (0.1 mV s^{-1}) for symmetric cells assembled with pristine or hybrid anodes; (b) Tafel plots obtained from analyzing results shown in (a); (c) Nyquist plots acquired from the symmetric cells and (d and e) analysis of the EIS results for the Li-ion diffusion coefficient and charge-transfer resistance; (f) rate capability of prototype full cells in which different Li anodes are paired with a NMC-811 cathode.

acquired at 0.1 mV s^{-1} within a voltage range of −0.1 to 0.1 V. They all exhibited linear shaped and symmetric polarization curves, suggesting dominance of the Li/Li^+ redox couple without obvious side redox reactions.[28] Importantly, both of the hybrid anodes exhibited steeper slopes that correspond to faster Li deposition/stripping kinetics compared with pristine Li anodes. The analysis of these results using the Tafel relationship yields their exchange current densities (Fig. 3b). The Mo_6S_8/C@Li anode had the best Li-ion charge transfer kinetics, evidenced with a substantially higher exchange current of 3.9 mA cm^{-2} compared with the Mo_6S_8@Li (1.5 mA cm^{-2}) and pristine Li (0.98 mA cm^{-2}) anodes.

The symmetric cells were also examined using electrochemical impedance spectroscopy (EIS) at open circuit potential and the obtained Nyquist plots are shown in Fig. 2c. These spectra were analyzed using the equivalent circuit model shown in Fig. S6† for estimation of charge-transfer resistance (R_{ct}), Warburg impedance (Z_w) and the Li-ion diffusion coefficient (D_{Li^+}). The Mo_6S_8/C@Li anode outperformed both Mo_6S_8@Li and pristine Li anodes, and exhibited the lowest charge transfer

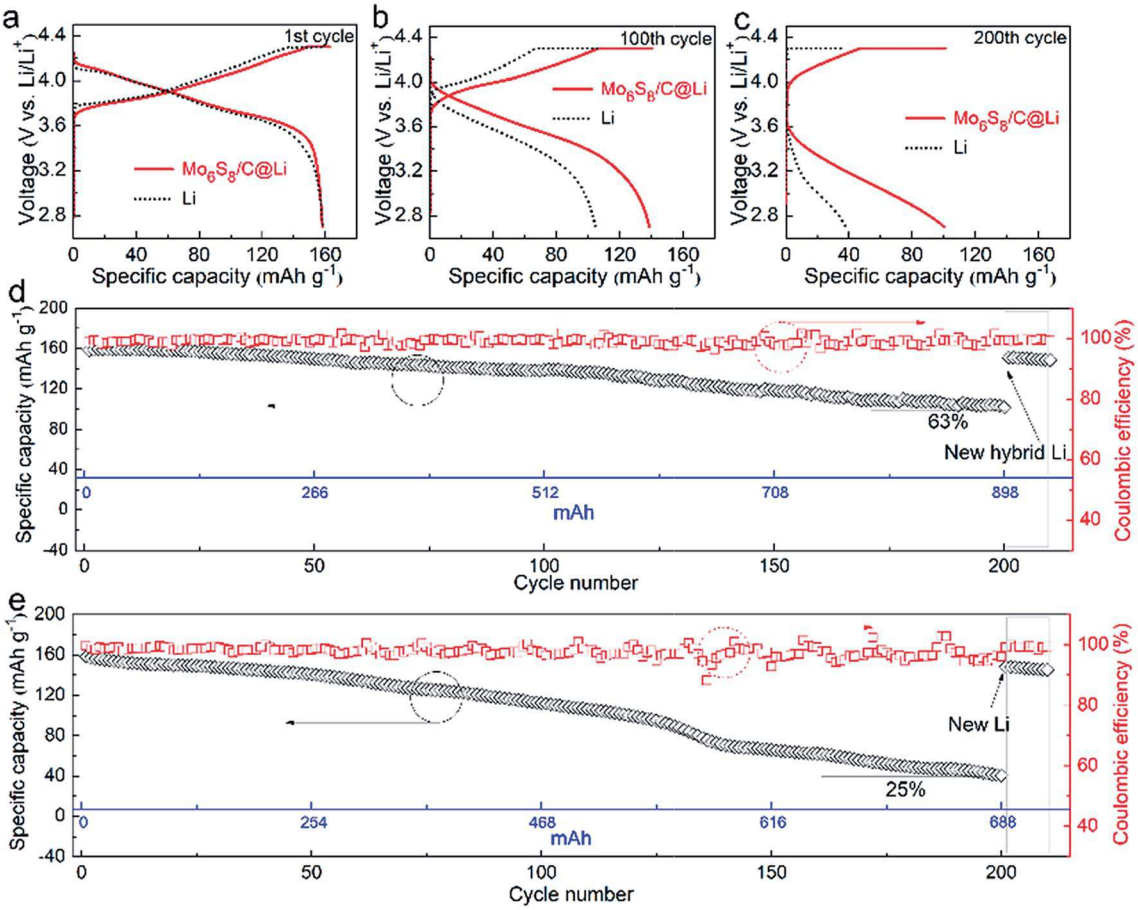

Fig. 3 Mo_6S_8/C@Li hybrid anodes significantly improved the cycling stability of Li metal batteries paired with the NMC-811 cathodes: comparison of voltage profiles at (a) the first, (b) 100th, and (c) 200th cycles; and cycling stability of full cells assembled with (d) hybrid Li anodes and (e) pristine Li anodes at 1.0C (1.52 mA cm^{-2}).

resistance of only 28 Ω cm^2 and the highest Li^+ diffusion coefficient that reached 2.7×10^{-11} cm^2 s^{-1} (Fig. 2e). The improved kinetics with the hybrid anodes also ensured Li metal batteries with much better rate performance. Specifically, different Li anodes were paired with the intercalation cathode $LiNi_{0.8}Mn_{0.1}Co_{0.1}O_2$ (NMC-811, coated on Al foil at 9.12 mg cm^{-2}). The cathodes were punched into relatively large discs (16 mm, 2.0 cm^2) and each disc delivered a capacity of ~3 mA h at 1C. The rate test shows that the Mo_6S_8/C@Li hybrid anode affords full cells with the best high rate performance (Fig. 2f), with 48% capacity retention the rate was increased to from 0.1 to 10C. In comparison, the Li||NMC-811 battery only had 35% retention. These results reinforce the conclusions drawn from the CV and EIS results that the Mo_6S_8/C artificial SEI layer promoted faster Li-ion transfer even though these films are relatively thick compared with typical SEI layers reported in the literature,[29–31] perhaps due to the inherent fast cation transport kinetics of the Chevrel phase compounds and/or the increased electrochemical active surface area with the introduction of Mo_6S_8/C nanoparticles.

The artificial SEI layers based on Mo_6S_8/C significantly improved the cycling stability of Li metal both in symmetric cell and full cell configurations. The symmetric cell with hybrid anodes only had slight polarization increases (up to 0.17 V) after 600 h of cycling at 1.0 mA cm^{-2} for 1.0 mA h cm^{-2} per cycle (Fig. S7†), which is much smaller than those of pristine Li anodes. The Li metal full cells were assembled with the same high-loading NMC-811 cathode and tested under 2.7–4.3 V for 200 cycles (Fig. 3). The NMC-811 is one of the most promising cathode materials but is poorly compatible with Li metal anode due to its reactivity with electrolytes that form corrosive intermediates to degrade Li metal.[32,33] The batteries were cycled at a current of 3.04 mA (equivalent to 1.52 mA cm^{-2}, 1C rate), which is usually considered an aggressive current because the degradation of Li metal is accelerated.[34] The battery with a hybrid anode delivered similar initial capacities to the one with pristine Li metal (at ~160 mA h g^{-1}) and their voltage profiles are nearly identical (Fig. 3a), indicating that the artificial SEI layers didn't affect the behavior of the Li anode, which agrees with observations from Fig. 2a. The capacity of both batteries decreased slowly during the first 100 cycles (Fig. 3d and e), and the hybrid anode afforded a smaller polarization increase and notably better stability, with a capacity retention of 88% as compared with the 71% for the pristine Li anode battery (Fig. 3b).

As the cycling continues a typical rapid capacity decay after ~120 cycles was observed for the battery with a pristine Li

anode due to nearly complete degradation of Li metal as previously described.[34,35] The coulombic efficiency (CE) also dropped to ~92% and the overall retention was only 25% (Fig. 3c). In contrast, the battery with the hybrid anode maintained highly efficient cycling (99.6% average CE) and had much better stability without abnormal decay, and overall retained 63% of the initial capacity after 200 cycles. Fig. 3d and e also compare the the sum of charging and discharging capacities cycled at Li anodes (blue colored *X*-axis). The hybrid anodes had superior stability and retained a total capacity of 898 mA h, which is among the best for Li metal protection under similar conditions.[8] In addition, it should be noted that the observed capacity decay originates mostly from the anode, as cells re-assembled with the same cathode but with fresh anodes and electrolytes recovered the initial capacities (Fig. 3). Furthermore, the impedance of these batteries was also determined during cycling (Fig. 4a and b). The R_{ct} was analyzed using the equivalent circuit model outlined in Fig. S8† and the results are included in the insets. Notably, the cell equipped with the hybrid anode had much better stability, and the R_{ct} increased from the initial 45 to 165 Ω cm^2 after 200 cycles. In strong contrast, the pristine Li anode reached to a much higher resistance of 425 Ω cm^2 after the same testing.

The effective protection of Li metal with artificial SEI layers was further confirmed with post-mortem analysis of Li anodes with EDS and SEM (Fig. 4, S9 and S10†). After 200 cycles, the SEI generated in the protected Li anode was much thinner (only ~20 μm) and the detected F and P concentrations were only half of those of the pristine Li anode (Fig. 4c and d). The surface of protected Li was also much smoother without obvious dendritic or mossy structures, whereas the pristine Li anode had a rather thick (~120 μm) SEI that appeared extremely porous (Fig. 4e–h, and S9 and S10† for additional SEM images). Notably, no Li growth was observed on the surface or within the bulk of the Mo_6S_8/C artificial SEI layers, suggesting that the presence of Mo_6S_8 didn't affect the growth behavior of Li metal. This is supported by the fact that the Li nucleation overpotential on lithiated Mo_6S_8 was rather high (~89 mV at 2 mA cm^{-2}) as shown in Fig. S11†[11,15] In addition, the artificial SEI layer maintained intimate contact with the metallic Li during battery cycling, as no segregation or peeling off was observed after 200 cycles (Fig. S12†). These combined electrochemical and post-mortem analyses therefore further strengthened the exceptional capability of the artificial SEI layers proposed in this work for isolation of Li and effectively mitigate its side-reactions with electrolyte, and provided significantly improved interfacial stability.

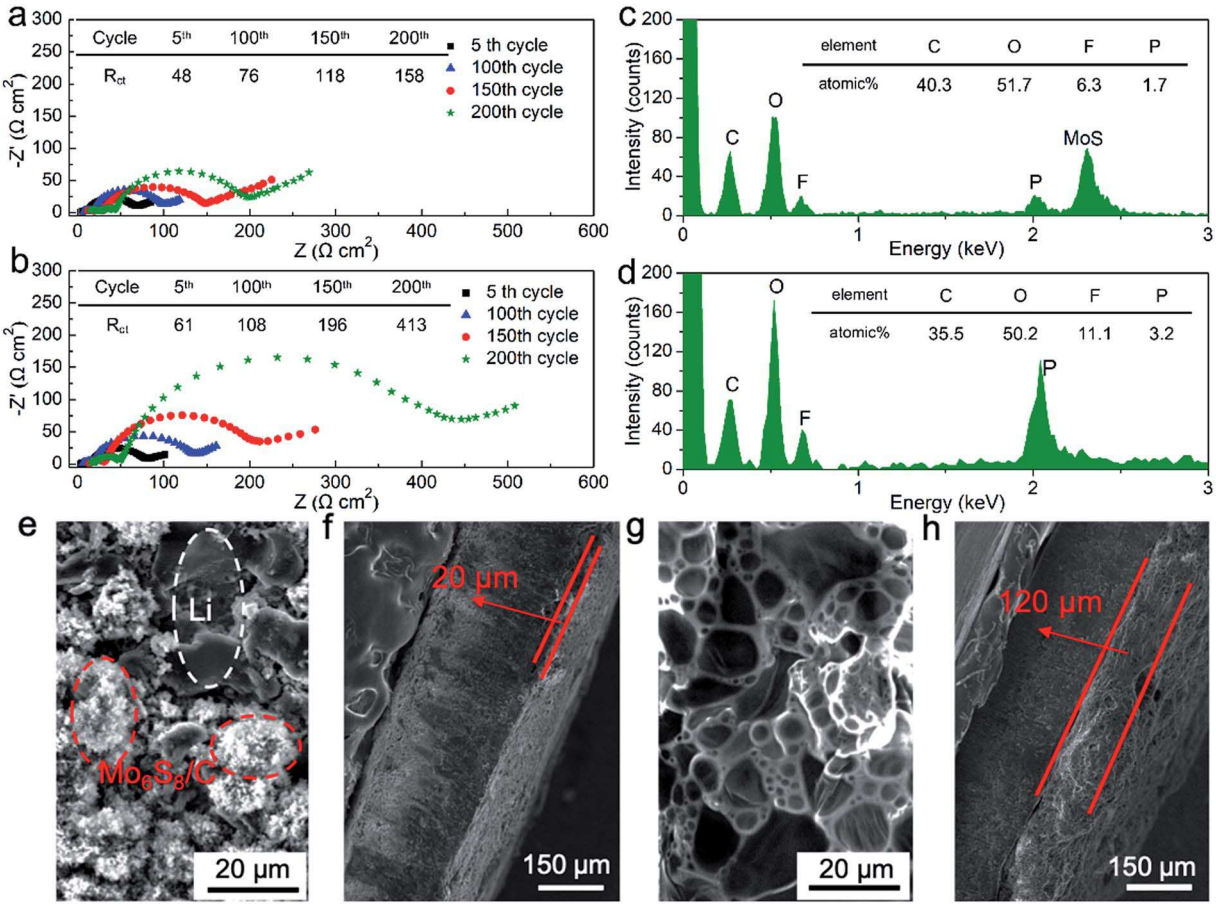

Fig. 4 Mo_6S_8/C artificial layers stabilize Li metal in carbonate electrolytes: Nyquist plot acquired for different stages of cycling for Li metal batteries with a (a) hybrid anode and (b) pristine Li anode; post-mortem (c and d) EDS spectra and (e–h) SEM images of the (c, e and f) hybrid anode and (d, g and h) pristine Li anode after 200 cycles with the NMC-811 cathodes.

In conclusion, we describe the design of transferrable artificial SEI layers using Mo_6S_8/C particles to improve the practical stability of Li metal in carbonate electrolytes. We discovered that Li anodes coated with Mo_6S_8/C films have substantially increased exchange current densities that could be attributed to the promoted and regulated Li-ion flux through the lithiated Mo_6S_8 frameworks. The $Li_{16}Mo_6S_8$/C films have intimate interaction with Li metal and protect it from parasitic reactions, which results in hybrid Li anodes that have stabilized interphases for practical applications as demonstrated with significantly improved cycling stability for prototype full cells coupled with high-loading NMC-811 cathodes.

Conflicts of interest

There are no conflicts to declare.

Acknowledgements

This work was supported by startup funds provided to Y. C. from Northern Illinois University. R. D. acknowledges the support from the U.S. National Science Foundation REU program, under Award CHE-1659548. Z. S. was a summer research volunteer from Bartlett High School in Bartlett, IL 60103. The NMC cathodes were produced at the U.S. Department of Energy's (DOE) CAMP (Cell Analysis, Modeling and Prototyping) Facility, Argonne National Laboratory. The CAMP Facility is fully supported by the DOE Vehicle Technologies Program (VTP) within the core funding of the Applied Battery Research (ABR) for Transportation Program.

References

1 X.-B. Cheng, R. Zhang, C.-Z. Zhao and Q. Zhang, Toward Safe Lithium Metal Anode in Rechargeable Batteries: A Review, *Chem. Rev.*, 2017, **117**(15), 10403–10473.
2 P. Albertus, S. Babinec, S. Litzelman and A. Newman, Status and challenges in enabling the lithium metal electrode for high-energy and low-cost rechargeable batteries, *Nat. Energy*, 2018, **3**(1), 16–21.
3 K. Lu, H. Zhang, S. Gao, H. Ma, J. Chen and Y. Cheng, Manipulating Polysulfide Conversion with Strongly Coupled Fe_3O_4 and Nitrogen Doped Carbon for Stable and High Capacity Lithium–Sulfur Batteries, *Adv. Funct. Mater.*, 2018, 1807309.
4 J. T. Vaughey, G. Liu and J.-G. Zhang, Stabilizing the surface of lithium metal, *MRS Bull.*, 2014, **39**(05), 429–435.
5 D. Aurbach, E. Zinigrad, Y. Cohen and H. Teller, A short review of failure mechanisms of lithium metal and lithiated graphite anodes in liquid electrolyte solutions, *Solid State Ionics*, 2002, **148**(3), 405–416.
6 B. Wu, S. Wang, J. Lochala, D. Desrochers, B. Liu, W. Zhang, J. Yang and J. Xiao, The role of the solid electrolyte interphase layer in preventing Li dendrite growth in solid-state batteries, *Energy Environ. Sci.*, 2018, **11**(7), 1803–1810.
7 P. Verma, P. Maire and P. Novák, A review of the features and analyses of the solid electrolyte interphase in Li-ion batteries, *Electrochim. Acta*, 2010, **55**(22), 6332–6341.
8 Y. Gao, Y. Zhao, Y. C. Li, Q. Huang, T. E. Mallouk and D. Wang, Interfacial Chemistry Regulation *via* a Skin-Grafting Strategy Enables High-Performance Lithium-Metal Batteries, *J. Am. Chem. Soc.*, 2017, **139**(43), 15288–15291.
9 W. Xu, J. Wang, F. Ding, X. Chen, E. Nasybulin, Y. Zhang and J.-G. Zhang, Lithium metal anodes for rechargeable batteries, *Energy Environ. Sci.*, 2014, **7**(2), 513–537.
10 E. Cha, M. D. Patel, J. Park, J. Hwang, V. Prasad, K. Cho and W. Choi, 2D MoS_2 as an efficient protective layer for lithium metal anodes in high-performance Li–S batteries, *Nat. Nanotechnol.*, 2018, **13**(4), 337–344.
11 J. Zhao, L. Liao, F. Shi, T. Lei, G. Chen, A. Pei, J. Sun, K. Yan, G. Zhou, J. Xie, C. Liu, Y. Li, Z. Liang, Z. Bao and Y. Cui, Surface Fluorination of Reactive Battery Anode Materials for Enhanced Stability, *J. Am. Chem. Soc.*, 2017, **139**(33), 11550–11558.
12 R. Xu, X.-Q. Zhang, X.-B. Cheng, H.-J. Peng, C.-Z. Zhao, C. Yan and J.-Q. Huang, Artificial Soft-Rigid Protective Layer for Dendrite-Free Lithium Metal Anode, *Adv. Funct. Mater.*, 2018, **28**(8), 1705838.
13 Q. Pang, X. Liang, I. R. Kochetkov, P. Hartmann and L. F. Nazar, Stabilizing Lithium Plating by a Biphasic Surface Layer Formed *In situ*, *Angew. Chem., Int. Ed.*, 2018, **57**(31), 9795–9798.
14 X. Liang, Q. Pang, I. R. Kochetkov, M. S. Sempere, H. Huang, X. Sun and L. F. Nazar, A facile surface chemistry route to a stabilized lithium metal anode, *Nat. Energy*, 2017, **2**(9), 17119–17124.
15 Z. Tu, S. Choudhury, M. J. Zachman, S. Wei, K. Zhang, L. F. Kourkoutis and L. A. Archer, Fast ion transport at solid–solid interfaces in hybrid battery anodes, *Nat. Energy*, 2018, **3**(4), 310–316.
16 Y. Liu, D. Lin, P. Y. Yuen, K. Liu, J. Xie, R. H. Dauskardt and Y. Cui, An Artificial Solid Electrolyte Interphase with High Li-Ion Conductivity, Mechanical Strength, and Flexibility for Stable Lithium Metal Anodes, *Adv. Mater.*, 2017, **29**(10), 1605531.
17 J. Liang, X. Li, Y. Zhao, L. V. Goncharova, G. Wang, K. R. Adair, C. Wang, R. Li, Y. Zhu, Y. Qian, L. Zhang, R. Yang, S. Lu and X. Sun, *In situ* Li_3 PS_4 Solid-State Electrolyte Protection Layers for Superior Long-Life and High-Rate Lithium-Metal Anodes, *Adv. Mater.*, 2018, e1804684.
18 N. W. Li, Y. X. Yin, C. P. Yang and Y. G. Guo, An Artificial Solid Electrolyte Interphase Layer for Stable Lithium Metal Anodes, *Adv. Mater.*, 2016, **28**(9), 1853–1858.
19 Q. Pang, X. Liang, A. Shyamsunder and L. F. Nazar, An *In vivo* Formed Solid Electrolyte Surface Layer Enables Stable Plating of Li Metal, *Joule*, 2017, **1**(4), 871–886.
20 N. D. Trinh, D. Lepage, D. Ayme-Perrot, A. Badia, M. Dolle and D. Rochefort, An Artificial Lithium Protective Layer that Enables the Use of Acetonitrile-Based Electrolytes in Lithium Metal Batteries, *Angew. Chem., Int. Ed.*, 2018, **57**(18), 5072–5075.

21 X.-Q. Zhang, X. Chen, X.-B. Cheng, B.-Q. Li, X. Shen, C. Yan, J.-Q. Huang and Q. Zhang, Highly Stable Lithium Metal Batteries Enabled by Regulating the Solvation of Lithium Ions in Nonaqueous Electrolytes, *Angew. Chem.*, 2018, **130**(19), 5399–5403.

22 M. S. Kim, J.-H. Ryu, Deepika, Y. R. Lim, I. W. Nah, K.-R. Lee, L. A. Archer and W. Il Cho, Langmuir–Blodgett artificial solid-electrolyte interphases for practical lithium metal batteries, *Nat. Energy*, 2018, **3**(10), 889–898.

23 E. Levi, G. Gershinsky, D. Aurbach, O. Isnard and G. Ceder, New Insight on the Unusually High Ionic Mobility in Chevrel Phases, *Chem. Mater.*, 2009, **21**(7), 1390–1399.

24 J. Yue, X. Zhu, F. Han, X. Fan, L. Wang, J. Yang and C. Wang, A Long-Cycle Life All-Solid-State Sodium Ion Battery, *ACS Appl. Mater. Interfaces*, 2018, **10**(46), 39645–39650.

25 P. Saha, P. H. Jampani, M. K. Datta, D. Hong, B. Gattu, P. Patel, K. S. Kadakia, A. Manivannan and P. N. Kumta, A rapid solid-state synthesis of electrochemically active Chevrel phases (Mo_6T_8; T = S, Se) for rechargeable magnesium batteries, *Nano Res.*, 2017, **10**(12), 4415–4435.

26 Y. Cheng, L. R. Parent, Y. Shao, C. Wang, V. L. Sprenkle, G. Li and J. Liu, Facile Synthesis of Chevrel Phase Nanocubes and Their Applications for Multivalent Energy Storage, *Chem. Mater.*, 2014, **26**(17), 4904–4907.

27 E. Lancry, E. Lancry, E. Levi, E. Levi, A. Mitelman, A. Mitelman, S. Malovany, S. Malovany, D. Aurbach and D. Aurbach, Molten salt synthesis (MSS) of $Cu_2Mo_6S_8$—New way for large-scale production of Chevrel phases, *J. Solid State Chem.*, 2006, **179**(6), 1879–1882.

28 A. C. Kozen, C.-F. Lin, A. J. Pearse, M. A. Schroeder, X. Han, L. Hu, S.-B. Lee, G. W. Rubloff and M. Noked, Next-Generation Lithium Metal Anode Engineering *via* Atomic Layer Deposition, *ACS Nano*, 2015, **9**(6), 5884–5892.

29 S. Wei, S. Choudhury, Z. Tu, K. Zhang and L. A. Archer, Electrochemical Interphases for High-Energy Storage Using Reactive Metal Anodes, *Acc. Chem. Res.*, 2018, **51**(1), 80–88.

30 Y. Li, Y. Sun, A. Pei, K. Chen, A. Vailionis, Y. Li, G. Zheng, J. Sun and Y. Cui, Robust Pinhole-free Li_3N Solid Electrolyte Grown from Molten Lithium, *ACS Cent. Sci.*, 2018, **4**(1), 97–104.

31 S. Xin, Y. You, S. Wang, H.-C. Gao, Y.-X. Yin and Y.-G. Guo, Solid-State Lithium Metal Batteries Promoted by Nanotechnology: Progress and Prospects, *ACS Energy Lett.*, 2017, **2**(6), 1385–1394.

32 M. Li, J. Lu, Z. Chen and K. Amine, 30 Years of Lithium-Ion Batteries, *Adv. Mater.*, 2018, e1800561.

33 Y. Yu, P. Karayaylali, Y. Katayama, L. Giordano, M. Gauthier, F. Maglia, R. Jung, I. Lund and Y. Shao-Horn, Coupled $LiPF_6$ Decomposition and Carbonate Dehydrogenation Enhanced by Highly Covalent Metal Oxides in High-Energy Li-Ion Batteries, *J. Phys. Chem. C*, 2018, **122**(48), 27368–27382.

34 J. Zheng, M. H. Engelhard, D. Mei, S. Jiao, B. J. Polzin, J.-G. Zhang and W. Xu, Electrolyte additive enabled fast charging and stable cycling lithium metal batteries, *Nat. Energy*, 2017, **2**, 17012.

35 D. Lu, Y. Shao, T. Lozano, W. D. Bennett, G. L. Graff, B. Polzin, J. Zhang, M. H. Engelhard, N. T. Saenz, W. A. Henderson, P. Bhattacharya, J. Liu and J. Xiao, Failure Mechanism for Fast-Charged Lithium Metal Batteries with Liquid Electrolytes, *Adv. Energy Mater.*, 2014, **5**(3), 1400993.

